Diffusion and localization in hierarchical potentials

S. Teitel
Department of Physics and Astronomy, University of Rochester, Rochester, New York 14627
(Received 21 November 1988)

A simple model of classical relaxation in a one-dimensional harmonic potential with a hierarchical distribution of barriers is studied. The vanishing of an effective diffusion constant results in a transition of the low-lying eigenstates of the master equation from extended to localized. For a parameter characterizing the barrier distribution greater than a critical value $R > R_c$, the low-lying states are extended on the length scale of the equilibrium distribution. For $R < R_c$ the low-lying states are sharply localized at the most difficult barriers to cross. The correlation function $\langle x(t)x(0)\rangle$ is analyzed in terms of this eigenstate structure. For $R > R_c$ correlations are shown to decay as a pure exponential for all times. For $R < R_c$, decay is a sum of exponentials which asymptotically approaches the stretched exponential form at long times. Numerical simulations are performed to compute the decay of the correlation functions at shorter times. This decay may also be empirically fitted to a stretched exponential form. The relation of the model to anomalous relaxation in glassy systems is discussed.

I. INTRODUCTION

Stretched exponential relaxation of the form $e^{-(t/\tau)^\beta}$ has been observed in a wide variety of experimental systems involving disordered materials. These include decay of remnant magnetization in spin glasses;[1] the decay of density fluctuations in dense microemulsions[2] and ionic glasses;[3] the relaxation of electric polarization in charge-density waves;[4] the relaxation of occupied band-tail states in amorphous semiconductors;[5] the relaxation of viscosity in plate glass;[6] thermal relaxation in *o*-terphenyl mixtures;[7] and the relaxation of proteins after changes in conformal state.[8] A common feature of most of these glassy systems is generally believed to be a large number of metastable states in which the system may get trapped. The barriers separating these local free-energy minima, which must be crossed by thermal activation as the system relaxes to equilibrium, introduce a broad distribution of microscopic time scales, leading to anomalously slow decay of correlations.[9]

Theoretically, stretched exponential relaxation has been found in many simple models. Ngai[10] has invoked the results of random matrix theory as the origin of the broad distribution of relaxation rates. Campbell *et al.*[11] have modeled the effects of free-energy barriers in phase space on relaxation in the Ising spin glass, by a random walk on a bond-diluted hypercube. Dotsenko[12] has modeled relaxation in spin glasses in terms of diffusion on a self-similar free-energy surface. Riera and Hertz[13] find a distribution of rates from a renormalization-group analysis of the Ising spin glass on a Berker lattice. Their results agree qualitatively with Monte Carlo simulations by Ogielski.[14] Huse and Fisher[15] have shown that stretched exponential relaxation exists[16,17] in the ordered phase of the ordinary two-dimensional ferromagnetic Ising model. In this case, while there is presumably no problem with metastable minima, the stretched decay is the result of slowly decaying excitations (large domains) far from equilibrium. Several models[18–26] introduce a distribution or hierarchy of time scales explicitly. Palmer *et al.*[18] consider hierarchically constrained glassy dynamics in which slow degrees of freedom can relax only after the faster processes have taken place. Huberman and Kerszberg[22] have introduced diffusion in ultrametric spaces[22–26] as a model of anomalously slow relaxation. However, for most of these models, stretched exponential relaxation results only for special choices of the rate distribution. A physical model, explaining the form of the distribution and how it might vary to produce a transition from simple to stretched exponential decay, is often lacking. Much work has also been done on the problem of diffusion in systems with energetic disorder,[27–34] and its relation to the glass problem. Analogies with the phenomenon of localization in quantum systems have been made.[35–37]

In this paper I discuss a simple microscopic model in which localization provides the physical mechanism for a transition to anomalously slow relaxation. I consider diffusion in a one-dimensional space on a complicated free-energy surface. The particle sits in a harmonic potential, having a well-defined global minimum and equilibrium distribution. However, a hierarchy of barriers is placed between sites, so that each site acts as a local energy minimum. Asymmetric hopping over the barriers due to thermal activation is the mechanism for relaxation to equilibrium. I find a dynamic transition from simple to stretched exponential relaxation, as a parameter controlling the barrier distribution is varied. The transition may be characterized as a localization transition of the lowest-lying eigenstates of the master equation, which occurs when an effective diffusion constant vanishes. The principle results have already been presented elsewhere;[38] here I provide details of the calculation, as well as several new results concerning the decay of correlation functions

in the anomalous region.

The rest of the paper is organized as follows. In Sec. II A the model is defined. In Sec. II B a derivation of the hopping rates used in the model is presented, which involves showing how to discretize the continuous dynamics of a diffusive Langevin equation. In Sec. II C the principle results of earlier work with a flat potential, and hence symmetric hopping rates, is summarized. Section III is concerned with an analysis of the low-lying states of the master equation. In Sec. III A the lowest nonzero eigenvalue is computed numerically, and explained in terms of scaling arguments. In Sec. III B a transition seen in the behavior of this lowest eigenvalue is explained in terms of a localization transition of the corresponding eigenvector. Section IV explains the effects of the eigenstate structure found in Sec. III, on the decay of correlation functions. In Sec. IV A it is shown that the asymptotic long-time behavior in the anomalous region approaches a stretched exponential. In Sec. IV B numerical simulations are used to calculate the decay of the correlation function at shorter times. Although in these simulations the times are too short for the results of Sec. IV A to apply, the data are empirically found to be reasonably approximated by a stretched exponential form. In Sec. V, I present a summary and discussion of the results.

II. DISCUSSION OF MODEL

A. Definition of model

The model I consider is illustrated in Fig. 1. A classical particle moves on a chain of sites $x=0,\pm1,\pm2,\ldots,\pm N/2$, where $N=3^n$ is the total length of the chain. At each instant in time the particle can hop from site x to sites $x\pm1$ with a transition rate $W_{x,x\pm1}$. The dynamics of the particle is specified by the master equation for the probability that the particle is at position x at time t:

$$\begin{aligned}\frac{dP(x)}{dt}&=W_{x+1,x}P(x+1)+W_{x-1,x}P(x-1)\\&\quad-(W_{x,x+1}+W_{x,x-1})P(x)\\&\equiv-\sum_{x}M_{x,x'}P(x')\ ,\end{aligned}\tag{2.1}$$

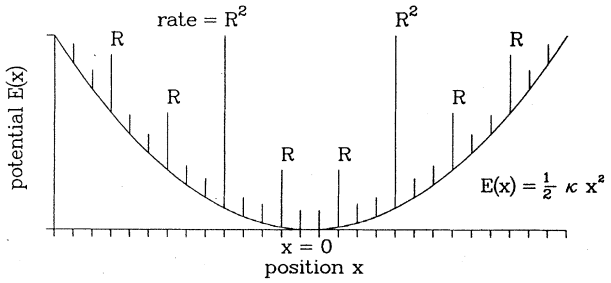

FIG. 1. Hierarchical barriers in a harmonic potential $E(x)$. The state of the system sits on integer sites x. To move right or left it must hop a barrier. These are arranged in a trifurcating hierarchical fashion, labeled by the rate $W^{(0)}=R^n$ to hop when the potential is flat, i.e., $\kappa=0$. Unlabeled barriers have rate $W^{(0)}=1$.

where $M_{x,x'}$ is the tridiagonal master equation matrix. The rates $W_{x,x\pm1}$ are determined by two effects.

(i) To cross from site x to $x\pm1$ the particle must hop a barrier. These barriers are arranged in a self-similar hierarchical fashion. The rate to hop the barrier in the *absence* of any external force is given by

$$W^{(0)}_{x,x\pm1}=W^{(0)}_{x\pm1,x}=R^{n(x)}\ ,\tag{2.2}$$

where $0\le R\le1$ and for $x\gtrless0$, $n(x)=n$ if $(2|x|\pm1)\bmod(3^l)=0$ for all $l\le n$ (see Fig. 1). Parametrizing these rates as

$$R^n=e^{-n\Delta_0/T}\tag{2.3}$$

one can view the hopping as thermal activation over a free-energy barrier whose height $n\Delta_0$ increases linearly with the level n of the hierarchy.

(ii) The particle feels a force from an external potential

$$E(x)=\tfrac{1}{2}\kappa_0 x^2\ .\tag{2.4}$$

This potential introduces an asymmetry into the transition rates which is fixed by detailed balance

$$\frac{W_{x,x\pm1}}{W_{x\pm1,x}}=e^{[E(x)-E(x\pm1)]/T}\ .\tag{2.5}$$

T is the temperature and I take $k_B=1$. The condition (2.5) guarantees that the equilibrium probability distribution for the particle to be at site x is given by the Gibb's distribution

$$P_{\rm eq}(x)\sim e^{-E(x)/T}\ .\tag{2.6}$$

It will be convenient to define a reduced coupling κ such that

$$\kappa\equiv\kappa_0/T\ .\tag{2.7}$$

Many choices of the rates $W_{x,x\pm1}$ would be consistent with detailed balance (2.5), which just fixes the rate ratios. I will choose rates such that the response of the system to the external force is that of overdamped diffusion. That is for the special case of equal barriers, $R=1$, the dynamics will be equivalent to a discretized version of the continuum Langevin equation[39]

$$\frac{dx}{dt}=-D_0\frac{dE}{dx}+\zeta(t)\ ,\tag{2.8}$$

where D_0 is a diffusion coefficient, and ζ is a thermal noise with correlation

$$\langle\zeta(t)\zeta(t')\rangle=2D_0T\delta(t-t')\ .$$

As I show in Sec. II B, the correct choice of rates that includes both the barrier hopping (2.2) and reduces to the Langevin dynamics (2.8) is

$$\begin{aligned}W_{x,x+1}&=R^{n(x)}e^{[E(x)-E(x+1)]/2T}\ ,\\W_{x+1,x}&=W_{x,x+1}e^{[E(x+1)-E(x)]/T}\ .\end{aligned}\tag{2.9}$$

One may view the above as a simplified model of a system diffusing in phase space on a complicated free-energy surface. Each site x represents a local free-energy minimum which is separated from the neighboring mini-

ma by a barrier. The barriers exist on all energy scales, and the dynamics is that of the system hopping from minimum to minimum, diffusing to the global minimum at $x=0$.

It will be useful to transform the master equation (2.1) to a symmetric form by the mapping[39]

$$\psi(x)\equiv e^{E(x)/2T}P(x)\ ,$$
$$\tilde{M}_{x,x'}\equiv e^{E(x)/2T}M_{x,x'}e^{-E(x')/2T}\ , \tag{2.10}$$

so that the equation of motion (2.1) becomes

$$\frac{d\psi(x)}{dt}=-\sum_{x'}\tilde{M}_{x,x'}\psi(x')\ . \tag{2.11}$$

Detailed balance (2.5) and the definition (2.1) of $M_{x,x'}$ ensure that $\tilde{M}_{x,x'}$ is a symmetric matrix. Its eigenvectors $\psi_i(x)$, with corresponding eigenvalues λ_i, therefore form a complete orthonormal basis in terms of which one can solve for the time evolution of the probability distribution of the system,

$$P(x,t)=\sum_i e^{-E(x)/2T}\psi_i(x) \times\sum_{x'}\psi_i^*(x')P(x',0)e^{E(x')/2T}e^{-\lambda_i t}\ . \tag{2.12}$$

The asymptotic long-time behavior is thus governed by the smallest eigenvalues of $\tilde{M}$.

B. Derivation of hopping rates

In this section I show how the rates $W_{x,x\pm1}$ given in Eq. (2.9) follow from the requirement that the master equation (2.1) model the dynamics of overdamped diffusion given by the continuum Langevin equation (2.8), in the limit of equal barriers ($R=1$). I begin by reviewing the solution for this continuum Langevin dynamics.

Using standard techniques,[39] one can derive from the Langevin equation (2.8) the corresponding Fokker-Planck equation for the probability distribution $P(x,t)$ that the system is at position x at time t. One has

$$\frac{\partial P(x)}{\partial t}=D_0\frac{\partial}{\partial x}\left[\frac{dE}{dx}P(x)\right]+D_0T\frac{\partial^2 P}{\partial x^2}\ . \tag{2.13}$$

This equation is the continuum analog of the master equation (2.1) for the discrete chain.

Making the transformation (2.10), $\psi(x)=e^{E(x)/2T}P(x)$, transforms the Fokker-Planck equation to an imaginary time Schrödinger equation,

$$\frac{\partial\psi}{\partial t}=-D_0T\left[V(x)\psi-\frac{\partial^2\psi}{\partial x^2}\right]\ , \tag{2.14}$$

where

$$V(x)=\left[\frac{E'(x)}{2T}\right]^2-\frac{E''(x)}{2T} \tag{2.15}$$

and primes denote derivatives with respect to x. The eigenfunctions $\psi_i(x)$ of this Schrödinger operator, together with their corresponding eigenvalues λ_i, then provide a basis for expanding the general solution for the probability distribution $P(x,t)$ as in Eq. (2.12).

For the harmonic potential $E(x)=\frac{1}{2}\kappa_0 x^2$, $V(x)=\frac{1}{4}\kappa^2x^2-\frac{1}{2}\kappa$, and so the problem reduces to the solution of the quantum harmonic oscillator. The eigenvalues are

$$\lambda_n=D_0T\kappa n,\quad n=0,1,2,\ldots \tag{2.16}$$

and the lowest two eigenfunctions are

$$\psi_0(x)=\left[\frac{\kappa}{2\pi}\right]^{1/4}e^{-\kappa x^2/4},\quad \psi_1(x)=\sqrt{\kappa}x\psi_0(x)\ . \tag{2.17}$$

As seen from the transformation (2.10), $\psi_0(x)$, with eigenvalue $\lambda_0=0$, is the eigenstate representing the equilibrium Gibb's probability distribution (2.6). $\tau\equiv1/\lambda_1\sim1/\kappa$ is the asymptotic decay time to equilibrium.

Returning to the original problem on the discrete chain, specified by the master equation (2.1) and its symmetric equivalent (2.11), we see what form the matrix $\tilde{M}$ must have if (2.11) is to represent a discretized version of the Schrödinger equation (2.14). Replacing $\partial^2/\partial x^2$ in (2.14) by its lattice equivalent results in

$$\frac{\partial\psi(x)}{\partial t}=-D_0T\{[V(x)-2]\psi(x)+\psi(x+1)+\psi(x-1)\}\ . \tag{2.18}$$

The matrix operator on the right-hand side of the above equation has constant off-diagonal elements, while the potential $E(x)$ enters only the diagonal elements through the term $V(x)$. We want $\tilde{M}$ to have this same form.

From the master equation (2.1) and the symmetrizing transformation (2.10) one can write down the matrix $\tilde{M}$ as

$$\tilde{M}_{x,x'}=e^{[E(x)-E(x')]/2T}W_{x',x}(\delta_{x',x+1}+\delta_{x',x-1}) -(W_{x,x+1}+W_{x,x-1})\delta_{x',x}\ . \tag{2.19}$$

The choice for $W_{x',x}$ needed to agree with (2.18) is therefore

$$W_{x',x}=D_0Te^{[E(x')-E(x)]/2T}\ . \tag{2.20}$$

The resulting off-diagonal terms are just the constant D_0T, while the resulting diagonal terms are

$$W_{x,x+1}+W_{x,x-1}=-D_0T(e^{[E(x)-E(x+1)]/2T}+e^{[E(x)-E(x-1)]/2T})\ . \tag{2.21}$$

Expanding the above to lowest order in $E(x)-E(x\pm1)$ reproduces the diagonal term in (2.18), $D_0T[V(x)-2]$, except that now discrete derivatives of $E(x)$ appear in defining $V(x)$ as in Eq. (2.15).

The above (2.20) are the correct rates to discretize the Langevin dynamics (2.8) for any potential $E(x)$ defined on a lattice. The generalization to higher dimensions is straightforward.

The above arguments assumed that the barriers between sites on the chain were equal ($R=1$), and that in the absence of any applied forces, i.e., $E(x)=$const, the rate to hop left or right is the constant D_0T independent of position x. To include the more general case we are in-

terested in, where $R<1$ and the barriers are not equal, I will assume that the natural extension to (2.20) is to replace this uniform rate D_0T by the local, spatially varying, barrier hopping rates $W^{(0)}_{x,x+1}=R^{n(x)}$ given in Eq. (2.2). The result is the rates given by Eq. (2.9) in Sec. II A. As before, the external potential enters the symmetrized master equation matrix $\tilde{M}$ in the diagonal elements only.

C. Flat potential $E(x)$=const

Much work[22,40–44] has been done on the special case $\kappa=0$. The potential $E(x)$ is constant, hopping rates are symmetric, $W_{x,x\pm1}=W_{x\pm1,x}$, and all sites are equally likely in equilibrium. In this section I review the results of this case, which are most easily stated in terms of the average diffusion constant of the system.[42]

A general result by Zwanzig[45] states that the asymptotic diffusion constant for any one-dimensional arrangement of N barriers with symmetric hopping rates is given by the average inverse hopping rate

$$\frac{1}{D(N)}=\frac{1}{N}\sum_x \frac{1}{W_{x,x+1}} . \tag{2.22}$$

For the rates of our model given by Eq. (2.2), and $N=3^n$, the sum can be written as a geometric series

$$\frac{1}{D(N)}=\frac{2}{3}\sum_{m=0}^{n-1}\frac{1}{(3R)^m} . \tag{2.23}$$

In the limit of $N\to\infty$ this sum yields

$$\begin{aligned} D(N\to\infty,R)&=\frac{3}{2}\left[1-\frac{1}{3R}\right] \quad \text{for } R>R_c=\tfrac{1}{3} , \\ D(N\to\infty,R)&=\frac{3}{2}\frac{1-1/3R}{1-(1/3R)^{\ln N/\ln 3}} \\ &\sim N^{1+\ln R/\ln 3}\to 0 \quad \text{for } R<R_c=\tfrac{1}{3} . \end{aligned} \tag{2.24}$$

For $R>R_c=\frac{1}{3}$ one gets ordinary diffusion

$$\langle x^2(t)\rangle\sim D(R)t \quad \text{for } R>R_c \tag{2.25}$$

with a diffusion constant $D(R)$ that goes linearly to zero as $R\to R_c$. For $R<R_c$, the asymptotic behavior can be obtained by the scaling argument

$$\langle x^2(t)\rangle\sim D(N\simeq x,R)t .$$

Using Eq. (2.24) for $D(N,R)$ and rearranging powers of x gives anomalously slow diffusion

$$\langle x^2(t)\rangle\sim t^{2\ln 3/(\ln 3-\ln R)} \quad \text{for } R<R_c , \tag{2.26}$$

where the exponent of the time dependence decreases continuously with R from a value of one at R_c.

The above scaling argument has been verified by various renormalization-group calculations.[40–44] The dynamical transition in the asymptotic long-time behavior of the average mean-square displacement, which occurs at $R_c=\frac{1}{3}$, can be thought of in the following way. For $R>R_c$, the time to go a distance x is determined by the average hopping time of all the barriers encountered in moving this distance. This average hopping time remains finite as x increases. For $R<R_c$, however, the time to go a distance x is dominated by the time to hop the most difficult barriers encountered.

III. LOW-LYING EIGENSTATES AND ASYMPTOTIC BEHAVIOR

In this section I return to the general model where $\kappa>0$, and the particle is affected by the force due to the external harmonic potential $E(x)$. We are interested to see how the hierarchical barriers will effect the decay of the particle to the global energy minimum at $x=0$, and what will be the manifestation of the dynamic transition discussed in Sec. II C for the force-free case.

A. Eigenvalues

As discussed at the end of Sec. II A, the asymptotic long-time behavior of the system will be determined by the low-lying eigenvalues of the symmetrized master equation matrix $\tilde{M}$. For the infinite system, if this spectrum of eigenvalues has a finite gap between the lowest two eigenvalues, $\lambda_0=0$ and λ_1, then at long enough times the decay will be exponential with a relaxation time $\tau=1/\lambda_1$. If the spectrum has a continuous distribution of eigenvalues as $\lambda\to 0$, the asymptotic decay may be slower than exponential.

I have numerically computed the smallest nonzero eigenvalue λ_1 of the matrix $\tilde{M}$ as a function of barrier parameter R and potential coupling κ for chains of sizes $N=3^6$–3^8. As $\tilde{M}$ is a symmetric tridiagonal matrix, the eigenvalues were easily and efficiently found by an algorithm based on use of the negative eigenvalue theorem[46] combined with a bisecting search. As the system size N increased for fixed R and κ, λ_1 reached a limiting nonzero value. Thus for finite κ, the infinite system has a finite gap to the lowest nonzero eigenvalue, and the true long-time asymptotic decay to equilibrium is always exponential. It will be shown in Sec. IV, however, that as $\kappa\to 0$, the asymptotic decay over long intermediate times is a stretched exponential.

The results for this asymptotic decay time $\tau=1/\lambda_1$ are plotted in Fig. 2 versus potential coupling κ for several values of the barrier parameter R. A least-squares fit (solid lines) to the form

$$\tau\sim B(R)\kappa^{-z(R)} \quad \text{as } \kappa\to 0 \tag{3.1}$$

gives excellent agreement. The exponent $z(R)$ thus obtained is shown in Fig. 3. In Fig. 4 is shown the scaling amplitude $B(R)$. The dots are the numerical results obtained from the least-squares fits to the data of Fig. 2. The dashed lines result from the predictions discussed below.

As is clearly seen in Fig. 3, the exponent $z(R)$ undergoes a transition at the critical value $R_c=\frac{1}{3}$. This is the same R_c as was found in the force-free case (Sec. II C). Empirically I find that

$$\begin{aligned} z(R)&=1 \quad \text{for } R_c\le R\le 1 , \\ z(R)&=-\ln R/\ln 3 \quad \text{for } 0\le R\le R_c . \end{aligned} \tag{3.2}$$

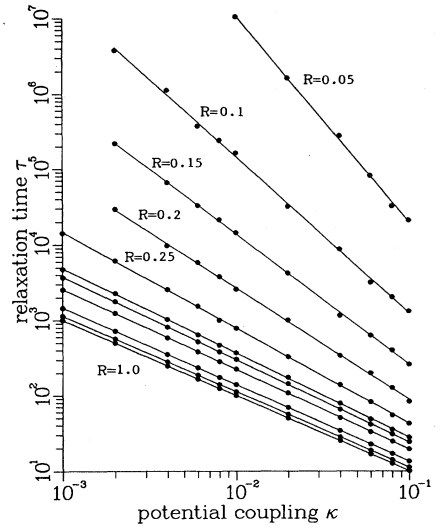

FIG. 2. Asymptotic relaxation time $\tau=1/\lambda_1$ vs κ for several values of barrier parameter R. The curves between $R=1$ and $R=0.25$ are for $R=0.8$, 0.6, and 0.4, $R_c=\frac{1}{3}$ and 0.3. Dots are numerically computed; solid lines are least-squares fits to the form $\tau=B(R)\kappa^{-z(R)}$.

The small disagreement from the above expressions observed in the neighborhood of R_c in Fig. 3 is due to finite-size effects from the fit to the form (3.1) at finite κ. For the values $R=0.3, R_c, 0.4$, calculations of the relaxation time τ were performed down to values of $\kappa=10^{-6}$ (the smaller κ the larger the chain size N needed to reach the $N\to\infty$ limiting value of λ_1). Fits to the form (3.1) at these lower values of κ produced a systematic decreasing in the value of the exponent z obtained, in better agreement with the expressions (3.2).

To explain the transition observed at R_c in the divergence of the relaxation time τ as $\kappa\to 0$, it is convenient to try a scaling argument as in Sec. II C. Assume that the

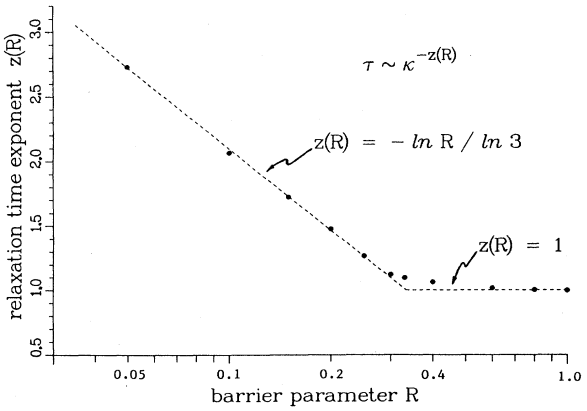

FIG. 3. Exponent $z(R)$ vs R. Dots are from least-squares fits to the data of Fig. 2. Dashed line is prediction $z(R)=1$ for $R>R_c$, $z(R)=-\ln R/\ln 3$ for $R<R_c=\frac{1}{3}$.

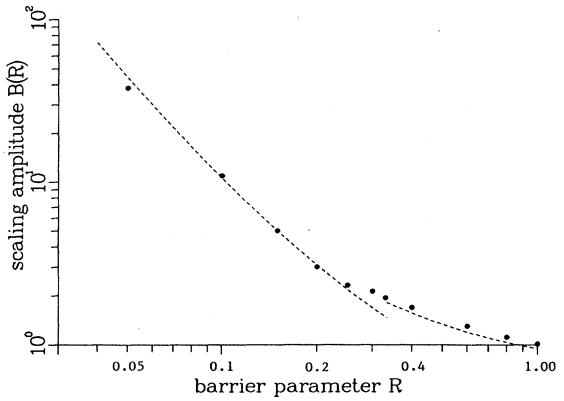

FIG. 4. Scaling amplitude $B(R)$ vs R. Dots are from least-squares fits to the data of Fig. 2. For $R<R_c=\frac{1}{3}$, the dashed line is the prediction from Eq. (3.9). For $R>R_c$, the dashed line is the prediction $B(R)=1/D(2L_{\rm eq},R)$ with $L_{\rm eq}=1/\sqrt{\kappa}$ evaluated at $\kappa=0.01$.

only effect of the barriers on relaxation in the potential is to provide an effective average diffusion constant $D(L)$. Here L is a length scale which depends on the potential coupling κ, that gives the effective size of the system sampled as the particle decays to $x=0$. $D(L)$ is the force-free diffusion constant from the barriers within this length L, as computed from Eq. (2.22). From the Langevin equation (2.8), the relaxation time would then be

$$\tau=1/D(L(\kappa))\kappa\ . \tag{3.3}$$

As $\kappa\to 0$, the potential becomes flatter, and one would expect the length $L(\kappa)\to\infty$. For $R>R_c$, as $L\to\infty$, $D(L)\to$const, so the relaxation time diverges as $\tau\sim 1/\kappa$. In this region therefore $z(R)=1$, as is the case for equal barriers ($R=1$). For $R<R_c$ however, as $L\to\infty$, $D(L)\to 0$ as $L^{1+\ln R/\ln 3}$ [see Eq. (2.24)]. If L diverges as a power of κ, $L\sim\kappa^{-y}$, then the relaxation time diverges as

$$\tau\sim L^{1+\ln R/\ln 3}\kappa\sim\kappa^{1-y-y\ln R/\ln 3}\ . \tag{3.4}$$

In order to agree with the numerical result (3.2), one therefore has to have $y=1$. The length scale L important for the asymptotic relaxation therefore varies with potential coupling κ as

$$L\sim 1/\kappa \quad \text{for } R<R_c\ . \tag{3.5}$$

This is to be compared with the naive guess for L, the equilibrium length scale of the Gibb's distribution $L_{\rm eq}=1/\sqrt{\kappa}$.

These results for exponent $z(R)$, scaling amplitude $B(R)$, and dynamic length scale $L(\kappa)$, can all be explained in terms of a simple Ansatz, motivated by the discussion of the force-free case in Sec. II C. I will assume that for $R>R_c$, the asymptotic decay is governed by the combined effects of all the barriers within a region $\sim\pm L_{\rm eq}=\pm 1/\sqrt{\kappa}$ of the global minimum at $x=0$. For $R<R_c$ however, I will assume that the asymptotic decay is determined by the singe most difficult barrier to cross.

This Ansatz leads to the following predictions.

(i) For $R > R_c$ the asymptotic decay time will be given by

$$\tau = 1/D(N \simeq 2L_{\rm eq}, R)\kappa, \quad R > R_c \ , \tag{3.6}$$

where $D(N,R)$ is computed from Eq. (2.22). The exponent is $z=1$ as $\kappa \to 0$. The scaling amplitude is $B(\kappa,R) = 1/D(2L_{\rm eq},R)$, and reaches a constant limiting value $1/D(R)$ as $\kappa \to 0$. These predictions are shown as the dashed lines at $R > R_c$ in Figs. 3 and 4. In Fig. 4, $B(R)$ is evaluated at the finite value $\kappa = 0.01$, the average of the values used in the data of Fig. 2. As $\kappa \to 0$, $B(R)$ should diverge as $R \to R_c$, due to the vanishing of $D(R_c)$. The absence of this divergence in Fig. 4 is due to the evaluation of $B(R)$ at finite κ.

(ii) For $R < R_c$ the asymptotic decay time is given by the inverse rate to hop the single most difficult barrier as the particle decays from finite x to $x=0$:

$$\tau = \max_{x>0}(1/W_{x+1,x}), \quad R < R_c \ . \tag{3.7}$$

Since the force-free barrier hopping rates $W^{(0)}_{x,x+1} = R^{n(x)}$ grow logarithmically with distance from the origin [$n(x) \sim \ln x / \ln 3$] while the force from the external harmonic potential $E(x)$ grows linearly with distance from the origin, there will be a well-defined most difficult barrier to cross. To maximize Eq. (3.7) it is sufficient to consider from the set of barriers of a given rate $W^{(0)} = R^m$, only that one which is closest to the origin $x=0$. As x increases, the first occurrence of the barrier with rate R^m occurs between sites $x = (3^m - 1)/2$ and $x+1$. Substituting this value of x into the expression (2.9) for the rates $W_{x+1,x}$, the maximization of (3.7) becomes the minimization with respect to m of $R^m \exp(\frac{1}{4}\kappa 3^m)$. This gives the most difficult barrier to cross occurring at position x_0, at level n_0 of the hierarchy,

$$x_0 \equiv \frac{3^{n_0}}{2} = -\frac{2}{\kappa}\frac{\ln R}{\ln 3} \ . \tag{3.8}$$

Thus we have the desired dynamic length scale $L \sim 1/\kappa$. Substituting x_0 back into the expression (2.9) for $W_{x+1,x}$ gives

$$\begin{aligned} \tau &= R^{-n_0 + 1/\ln 3} \\ &= \kappa^{\ln R/\ln 3} \exp\{(-\ln R/\ln 3) \\ &\qquad \times [\ln(-4\ln R/\ln 3) - 1]\} \ . \end{aligned} \tag{3.9}$$

The exponent of the diverging κ dependence is thus $z(R) = -\ln R/\ln 3$, as found empirically. The scaling amplitude $B(R)$ may also be read off from (3.9) and is plotted in Fig. 4 as the dashed line for $R < R_c$.

As seen in Figs. 3 and 4, the agreement of these predictions with the numerical results is excellent.

B. Eigenvectors and localization

The above analysis of the lowest nonzero eigenvalue λ_1 indicates a transition at R_c from dynamics governed by the average barrier to dynamics governed by the most difficult barrier. This can be more directly seen by a study of the eigenvectors $\psi_i(x)$ of the symmetrized master equation matrix $\tilde{M}$. The spatial dependence of the eigenvectors will give information about the barriers and length scales important to the asymptotic dynamic behavior.

I have numerically computed the eigenvector $\psi_1(x)$ corresponding to the lowest nonzero eigenvalue λ_1, for several values of R and κ. The eigenvectors were found using the NAG scientific library routine F02BEF and then iterated multiplicatively by $\tilde{M}$ to check for stability.

In Fig. 5 is plotted $\psi_1(x)$ for the case $R = 0.4 > R_c$, for a few decreasing values of the potential coupling κ (only $x \geq 0$ is shown; ψ_1 is antisymmetric about the origin). At the higher values of κ, the eigenvector takes discrete jumps at various tall barriers. However, in the limit $\kappa \to 0$, it is seen that $\psi_1(x)$ approaches the form expected for the equal barrier continuum case given by Eq. (2.17). This continuum solution is shown by the dashed line in Fig. 5. The length scale over which $\psi_1(x)$ is extended is the equilibrium length $L_{\rm eq} = 1/\sqrt{\kappa}$. As $L_{\rm eq}$ gets larger than the length on which $D(R)$ approaches its $N \to \infty$ limit, the spatially varying barriers may be effectively replaced by a uniform average barrier. Thus in the limit

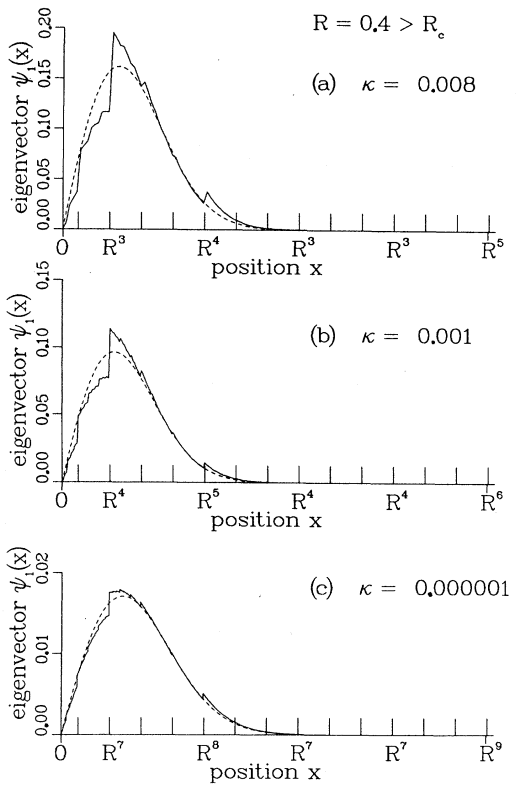

FIG. 5. Eigenvector $\psi_1(x)$ for the lowest nonzero eigenvalue, evaluated at $R = 0.4 > R_c$, at decreasing values of κ. ψ_1 is antisymmetric about the origin; only the positive x half is shown. The x axis is labeled by the locations of the various barriers in the hierarchy. The dashed line is the continuum (equal barrier) solution given by Eq. (2.17), which becomes an increasingly better approximation in the limit $\kappa \to 0$. The peak occurs at a position $x_{\rm peak} = \sqrt{2/\kappa} \sim L_{\rm eq}$.

$\kappa \to 0$ one expects the model to behave identically to an equal barrier model with uniform hopping rate $W^{(0)}_{x,x\pm1} = D(R)$.

In Fig. 6 is shown $\psi_1(x)$ for the case $R = 0.285 < R_c$, for a few decreasing values of κ. At the higher values of κ, $\psi_1(x)$ has a similar form to that of Fig. 5, with discrete jumps at tall barriers. However, now as $\kappa \to 0$ the behavior is radically different from the $R > R_c$ case. The eigenvector $\psi_1(x)$, instead of approaching the equal barrier form, becomes sharply localized at the most difficult barrier to cross, located at $\pm x_0 \sim 1/\kappa$ given by Eq. (3.8).

One can further verify the correctness of this localization of the lowest-lying, nonequilibrium, state ψ_1 by performing the following variational calculation. Take as a trial eigenvector the form

$$\psi^{(m)}(x) = \begin{cases} \dfrac{-1}{\sqrt{A}} e^{-E(x)/2T} & \text{for } x < -x_m \\ 0 \quad \text{for } -x_m \le x \le x_m \\ \dfrac{+1}{\sqrt{A}} e^{-E(x)/2T} & \text{for } x > x_m \ , \end{cases} \tag{3.10}$$

where A is the normalization constant

$$A = 2 \sum_{x > x_m} e^{-E(x)/T} .$$

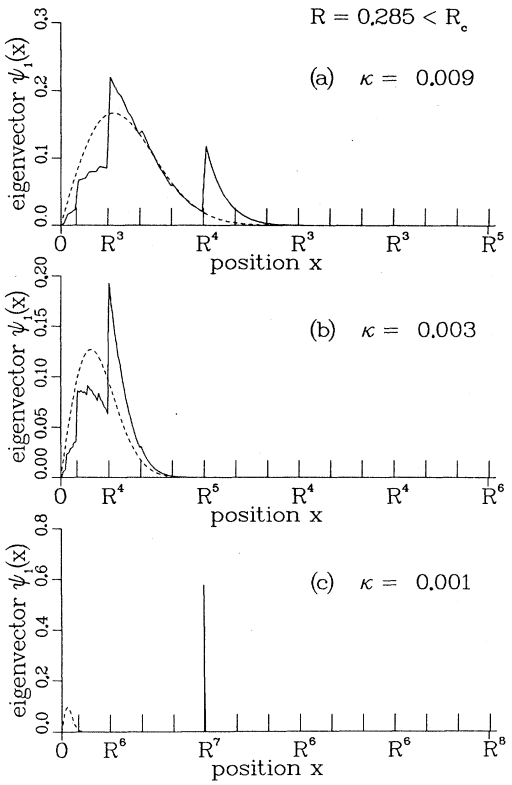

FIG. 6. Eigenvector $\psi_1(x)$ for the lowest nonzero eigenvalue, evaluated at $R = 0.285 < R_c$, at decreasing values of κ. ψ_1 is antisymmetric about the origin; only the positive x half is shown. The dashed line is the continuum (equal barrier) solution given by Eq. (2.17). As $\kappa \to 0$, ψ_1 localizes at the most difficult barrier to cross, located at a position $x_0 \sim 1/\kappa$, far from equilibrium, $L_{eq} \sim 1/\sqrt{\kappa}$.

Vary this trial eigenvector over the integers m, where $x_m = (3^m - 1)/2$ is the location of the first occurrence of a barrier of rate R^m. The variational eigenvalue thus obtained is

$$\lambda_1^{(\mathrm{var})} = \min_m \sum_{x,x'} \psi^{(m)}(x') \tilde{M}_{x',x} \psi^{(m)}(x)$$
$$= \min_m \left\{ \frac{R^m 2 e^{-[E(x_m+1)+E(x_m)]/2T}}{A} \right\} . \tag{3.11}$$

I have performed this variational minimization numerically. In Table I is shown the exact eigenvalue λ_1 and the variational value $\lambda_1^{(\mathrm{var})}$ for several values of $R < R_c$ at several decreasing values of κ. As $\kappa \to 0$, the variational calculation is approaching the exact answer to within arbitrary accuracy.

For $R < R_c$ it is interesting to examine the next lowlying eigenstates. Since ψ_1 was antisymmetric about $x = 0$, ψ_2 will be symmetric. However since $\psi_1(x) \to 0$ in a finite neighborhood of $x = 0$ as $\kappa \to 0$, ψ_2 will just be the symmetric transpose of ψ_1, $\psi_2(x) = \mathrm{sgn}(x)\psi_1(x)$. Thus $\lambda_2 \to \lambda_1$ as $\kappa \to 0$, and the eigenvalues become doubly degenerate. It is thus sufficient to consider only the odd numbered, antisymmetric eigenvectors. In Fig. 7 are plotted the states $\psi_1, \psi_3, \ldots, \psi_9$ and for the values $R = 0.25$ and $\kappa = 0.002$. ψ_1 is localized at the most difficult barrier to cross, at x_0. ψ_3 is localized at the second most difficult barrier, at $x_1 = x_0/3$. ψ_5, ψ_7, etc. are localized at the third, fourth, etc. most difficult barrier to cross. The sequence of localized states continues until the barrier of interest is located within a distance $\sim L_{eq}$ of the origin, and then the state becomes extended about the origin with width $\sim L_{eq}$. For comparison, the dashed lines in Figs. 7(d) and 7(e) represent the continuum (equal barrier) solutions ψ_1 and ψ_3, respectively.

IV. CORRELATION FUNCTIONS AND DYNAMIC TRANSITION

In this section I show how the structure of the lowlying eigenstates discussed in Sec. III gives rise to a dynamic transition in the decay of the position correlation function of the particle. I show that for $R > R_c$, as $\kappa \to 0$, decay is a pure exponential over all times. For $R < R_c$, as $\kappa \to 0$, decay is the sum of many exponentials over long intermediate times, which asymptotically approaches the stretched exponential form.

TABLE I. Comparison of numerically computed lowest nonzero eigenvalue λ_1 with values $\lambda_1^{(\mathrm{var})}$ from the variational calculation of Eq. (3.11).

$R = 0.285$	λ_1	$\lambda_1^{(\mathrm{var})}$	% error
$\kappa = 0.1$	3.302×10^{-2}	3.647×10^{-2}	10.0
$\kappa = 0.01$	2.416×10^{-2}	2.453×10^{-2}	1.5
$\kappa = 0.001$	1.756×10^{-3}	1.757×10^{-3}	0.07
$R = 0.25$	λ_1	$\lambda_1^{(\mathrm{var})}$	% error
$\kappa = 0.01$	1.267×10^{-2}	1.274×10^{-2}	0.55
$\kappa = 0.001$	7.017×10^{-4}	7.021×10^{-4}	0.057

A. Correlation function and eigenstate structure

Consider the position correlation function

$$\langle x(t)x(0)\rangle = \sum_{x,x_0} xx_0 P(x,t|x_0,0)P_{\rm eq}(x_0)\ , \tag{4.1}$$

where $P(x,t|x_0,0)$ is the probability for the particle to be at position x at time t, given it was at position x_0 at time $t=0$, and $P_{\rm eq}$ is the equilibrium distribution (2.6). Using Eq. (2.12) with the initial distribution $P(x',0)=\delta_{x',x_0}$ to compute $P(x,t|x_0,0)$, we get

$$\langle x(t)x(0)\rangle = \sum_i a_i e^{-\lambda_i t},\quad a_i = \left|\sum_x x\psi_0(x)\psi_i(x)\right|^2 , \tag{4.2}$$

where ψ_0 is the eigenstate with $\lambda_0=0$ corresponding to equilibrium, $\psi_0(x)=e^{-E(x)/2T}/\sqrt{Z}$, $Z=\sum_x e^{-E(x)/T}$. Since ψ_0 is symmetric about the origin, only antisymmetric ψ_i will give a nonzero coefficient a_i and contribute to the correlation function sum (4.2).

For $R>R_c$, it was shown in Sec. II B that as $\kappa\to 0$, the eigenvector $\psi_1(x)$ approaches the equal barrier continuum solution Eq. (2.17), $\psi_1(x)=\sqrt{\kappa}x\psi_0(x)$. Hence we can write for the coefficients, $a_i=|\sum_x \psi_1(x)\psi_i(x)|^2/\kappa$. The orthogonality of the eigenvectors then implies that only $a_1=1/\kappa$ is nonzero and so the correlation function is

$$\langle x(t)x(0)\rangle = \frac{1}{\kappa}e^{-\lambda_1 t} \tag{4.3}$$

decaying over all time as a pure exponential with relaxation time $\tau=1/\lambda_1$.

For $R<R_c$, however, $x\psi_0$ is no longer an eigenvector, so many if not all of the a_i are nonzero. The decay is given by a sum of exponentials. As $\kappa\to 0$, the low-lying eigenstates are localized at the most difficult barriers to cross. The terms which dominate the sum (4.2) at long times will come from states localized by the barriers at $x_m=x_0/3^m$ where x_0 is the most difficult barrier to cross given by Eq. (3.8), $x_0\equiv 3^{n_0}/2=-2\ln R/\kappa\ln 3$. If we approximate these localized eigenstates by δ functions we have

$$a_{m+1}=x_m^2\psi_0^2(x_m)\sim x_m^2 e^{-\kappa x_m^2/2},\quad x_m=x_0/3^m\ . \tag{4.4}$$

The eigenvalue λ_{m+1} is just the rate to hop the barrier at x_m. From Eq. (2.9) we have

$$\begin{aligned}\lambda_{m+1}&=R^{n_0-m}e^{[E(x_m+1/2)-E(x_m-1/2)]/T}\\ &=R^{n_0-m}e^{\kappa x_0 3^{-m}/2}\end{aligned} \tag{4.5}$$

and using $x_0=-2\ln R/\kappa\ln 3$ gives

$$\lambda_{m+1}=R^{n_0-m-(1/3^m\ln 3)}\ . \tag{4.6}$$

The term $(1/3^m\ln 3)$ in the exponent of R above rapidly becomes a negligible correction as m increases, so except at the longest time where small m terms dominate the sum (4.2), we can ignore it. Inserting Eqs. (4.4) and (4.6) into (4.2) then gives

$$\langle x(t)x(0)\rangle \sim \sum_{m=0} x_m^2 e^{-(\kappa x_0^2 3^{-2m}/2+tR^{n_0-m})}\ . \tag{4.7}$$

As $\kappa\to 0$, the asymptotic decay time $\tau=1/\lambda_1\to\infty$. For large $t<\tau$, we can approximate the sum over m in (4.7) by the saddle-point term at

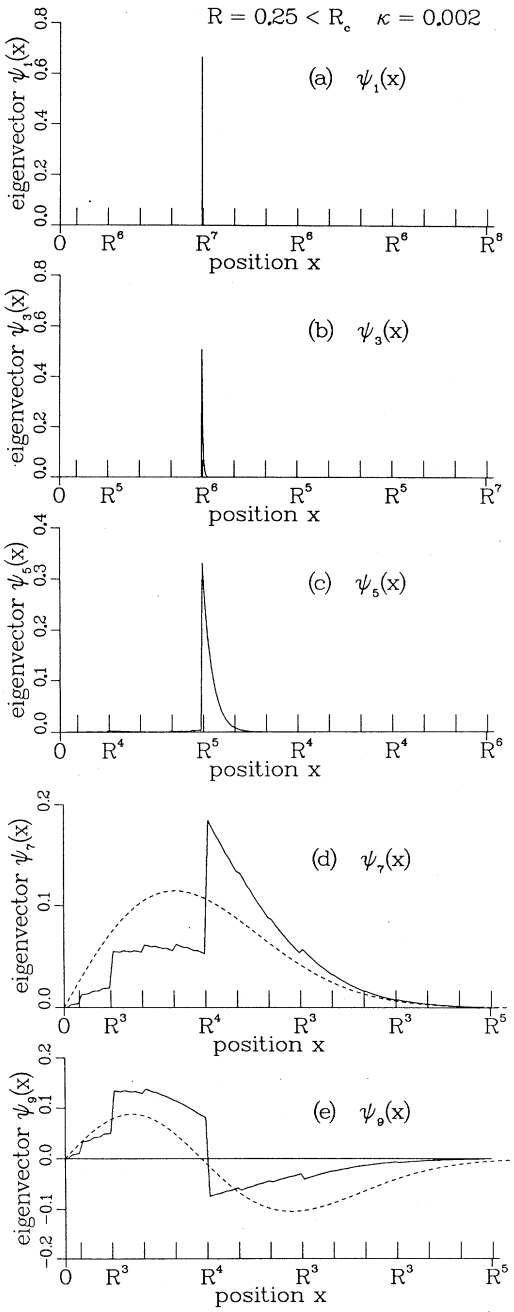

FIG. 7. Lowest five antisymmetric eigenvectors, evaluated at $R=0.25<R_c$ and $\kappa=0.002$. The first three, ψ_1, ψ_3, and ψ_5, are localized at the three most difficult barriers to cross, located at positions x_0, $x_0/3$, and $x_0/3^2$. The fourth and fifth, ψ_7 and ψ_9, are located with an equilibrium length of the origin, and so are more greatly extended. The dashed lines in (d) and (e) are the continuum (equal barrier) solutions for the two lowest antisymmetric states ψ_1 and ψ_3.

$$m^* = \ln\left[\left[\frac{-\ln R}{\ln 3}\right]\left[\frac{R^{n_0}}{\kappa x_0^2}\right]t\right]\Big/\ln\left[\frac{R}{3^2}\right] \tag{4.8}$$

yielding a stretched exponential form

$$\langle x(t)x(0)\rangle \sim \left[\frac{t}{\bar{\tau}}\right]^{\beta} e^{-(t/\bar{\tau})^{\beta}} \tag{4.9}$$

with

$$\beta(R) = \frac{2\ln 3}{2\ln 3 - \ln R} \tag{4.10}$$

and

$$\bar{\tau} = \left[\frac{\kappa x_0^2}{2}\left[1 - \frac{2\ln 3}{\ln R}\right]\right]^{-1/\beta}\left[\frac{-\ln 3}{\ln R}\right]R^{-n_0}\kappa x_0^2 \ . \tag{4.11}$$

At the critical value $R_c = \frac{1}{3}$, Eq. (4.10) gives $\beta(R_c) = \frac{2}{3}$. Thus β jumps discontinuously from 1 at $R > R_c$, to $\frac{2}{3}$ at $R = R_c$, and then decreases continuously to zero for $R < R_c$. Had we considered a p-branching hierarchy of barriers, instead of the tribranching hierarchy considered above, the only change is that the relevant barriers now occur at positions $x_m = x_0/p^m$. Now one finds $\beta(R) = 2\ln p/(2\ln p - \ln R)$. However, calculation of the diffusion constant (2.22) as in Sec. II C, shows[44] that the critical value is now $R_c = 1/p$. So $\beta(R_c) = \frac{2}{3}$ independent of the branching ratio p.

Having demonstrated that the decay approaches a stretched exponential at large $t < \tau \to \infty$, it is important to consider how long it takes until this stretched exponential form is reached. Using Eq. (3.8), $x_0 \equiv 3^{n_0}/2 = -2\ln R/\kappa \ln 3$, one can rewrite Eq. (4.11) in the form

$$\bar{\tau} = R^{-n_0/2}\beta(R)^{1/\beta(R)} \tag{4.12}$$

with $\beta(R)$ given by Eq. (4.10). Comparing with Eq. (3.9) for the true asymptotic exponential relaxation time $\tau = R^{-n_0 + 1/\ln 3}$ we see that for fixed R,

$$\bar{\tau} \sim \sqrt{\tau} \ . \tag{4.13}$$

In order for the analysis above which derived the stretched exponential to be valid, it is necessary that we be considering times large enough that $t\lambda_{m+1} \sim 1$ for m representing some localized eigenstate. Otherwise, if $t\lambda_{m+1} \ll 1$ for all localized states, relaxation will be governed by the eigenstates with shorter relaxation times $1/\lambda$ which are extended about the origin on the equilibrium length scale, and so Eqs. (4.4)–(4.6) will no longer apply. From Eqs. (4.6) and (3.9) we have $\lambda_{m+1} \simeq R^{n_0 - m}$ so the condition for the stretched exponential form to apply becomes $t \sim R^{m - n_0}$, or using Eq. (4.12), t must be large enough that

$$t/\bar{\tau} > R^{m_{\max} - n_0 + n_0/2}\beta^{-1/\beta} \ , \tag{4.14}$$

where $3^{n_0 - m_{\max}}/2$ is the position of the localized eigenstate closest to the origin. If we estimate this to occur at a distance $\sim 3L_{\rm eq} = 3/\sqrt{\kappa}$, use Eq. (3.8) for n_0, and (4.10) for β, we get the requirement

$$t/\bar{\tau} > \left[\frac{-\ln R}{9\ln 3}\right]^{\ln R/2\ln 3}\left[1 - \frac{\ln R}{2\ln 3}\right]^{1 - \ln R/2\ln 3} \tag{4.15}$$

in order for the stretched exponential derived above to apply. For values of $R = 0.3$, 0.2, 0.1, and 0.05, one gets $t/\bar{\tau} > 6.2$, 9.8, 20, and 39, respectively. As R decreases, one must wait times an order of magnitude or more greater than $\bar{\tau}$ in order to see the stretched exponential form $e^{-(t/\bar{\tau})^{\beta}}$. Thus in fitting data to this form one should fit only in the long-time tail of the correlation function, and not at shorter times $t \sim \bar{\tau}$.

B. Simulation of correlation function

Since the stretched exponential behavior derived in Sec. IV A above was shown to apply only at relatively long times $t > \bar{\tau}$, it is interesting to see how the correlation function decays at shorter times. I have therefore performed numerical simulations to directly compute the correlation function $\langle x(t)x(0)\rangle$. I have chosen a particular model where the parameters κ and R may be related to temperature T in a natural way

$$\kappa = \kappa_0/T, \quad R = e^{-\Delta_0/T} \tag{4.16}$$

so that

$$\kappa = -\frac{\kappa_0}{\Delta_0}\ln R \ . \tag{4.17}$$

This choice corresponds to a model with no equilibrium phase transition[47] at finite T, however, we expect a dynamic transition at $T_c = -\Delta_0/\ln R_c$. For such a model, combining Eqs. (4.17) and (3.8) gives the most difficult barrier to cross occurring at

$$x_0 \equiv \frac{3^{n_0}}{2} = \frac{2\Delta_0}{\kappa_0 \ln 3} \tag{4.18}$$

independent of temperature. The true asymptotic relaxation time at low temperatures τ, Eq. (3.9), behaves as

$$\exp\left\{-\Delta_0\left[\ln\left[\frac{\kappa_0}{4\Delta_0}\ln 3\right] + 1\right]\Big/T\right\} \tag{4.19}$$

and diverges with an Arrhenius form as $T \to 0$, provided $\kappa_0/\Delta_0 < 4e^{-1}/\ln 3$.

I have numerically simulated a particle taking a one-dimensional random walk with hopping rates given by Eq. (2.9) with (4.17). In order to have decay times sufficiently short that reasonable statistics could be obtained, I have chosen a value $\kappa_0/\Delta_0 = 0.01$. The initial position of the particle was selected randomly from the equilibrium distribution (2.6). At each update, the particle was moved one step to the right with probability $p = W_{x,x+1}/(W_{x,x+1} + W_{x,x-1})$ or one step to the left with probability $q = 1 - p$. After each update the time was advanced by $\Delta t = 1/W_{x,x\pm 1}$ according to whether the particle moved right or left. Thus a trajectory $x(t_i)$ was generated. The correlation function $\langle x(t)x(0)\rangle$ was computed by averaging over 50 000 independent random walks on a 3^8 site chain. Results, showing the decay of the correlation function versus $\ln t$, are given in Fig. 8 for

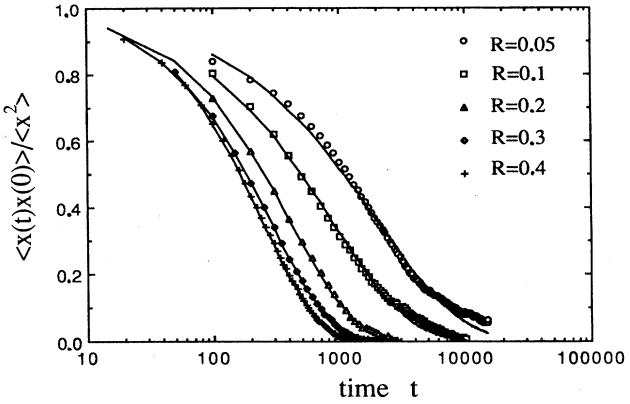

FIG. 8. Correlation function $\langle x(t)x(0)\rangle/\langle x^2\rangle$ vs ln$t$ from numerical simulations, for the values $R=0.4$, 0.3, 0.2, 0.1, and 0.05. The solid lines are empirical fits to a stretched exponential form.

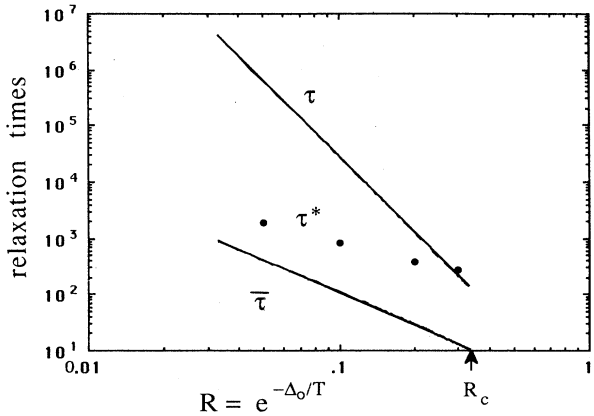

FIG. 10. Time scales of the numerically simulated model vs $-\ln R \sim 1/T$. $\tau=1/\lambda_1$ is the true asymptotic exponential decay time given by the time to hop the most difficult barrier, Eq. (3.9). $\bar{\tau}$ is the decay time of the long-time stretched exponential given by Eq. (4.12). τ^*, shown as dots, is the decay time of the stretched exponential empirically fitted at shorter times, to the data in Figs. 8 and 9. τ^* diverges with an apparent Arrhenius form.

several values of R from 0.3 to 0.05.

For the value $\kappa_0/\Delta_0=0.01$, Eq. (4.18) gives the most difficult barrier at $n_0=5$ or $x_0=121$. The equilibrium length $L_{\rm eq}=1/\sqrt{\kappa}$ varies between 9.1 at $R=0.3$ and 5.8 at $R=0.05$. Thus there are at most three relevant localized states, and it is questionable whether the approximations of Sec. IV A are applicable. Further, at the smallest R's where the states are most sharply localized, Eq. (4.15) would give the predicted stretched exponential behavior only at times much longer than were achieved in the simulation. Nevertheless, we can still empirically fit the decays of Fig. 8 to a stretched exponential form $e^{-(t/\tau^*)^{\beta^*}}$ for the range of t shown. In Fig. 9 I show the results of fits of $\ln\{-\ln[\langle x(t)x(0)\rangle/\langle x^2\rangle]\}$ to a straight line, determining the empirical τ^* and β^*. These fits are shown as solid lines in Fig. 8. The resulting decay times τ^* are plotted in Fig. 10, together with the true asymptotic exponential decay time τ of Eq. (4.19) and the asymptotic stretched exponential decay time $\bar{\tau}$ of Eq. (4.12) for comparison. The empirical τ^* has an apparent Arrhenius behavior. The resulting parameter β^* is shown in Fig. 11, with $\beta(R)$ from Eq. (4.10) for comparison. $\beta^*=1$ for $R>R_c$ and decreases continuously below R_c, with no apparent jump at R_c.

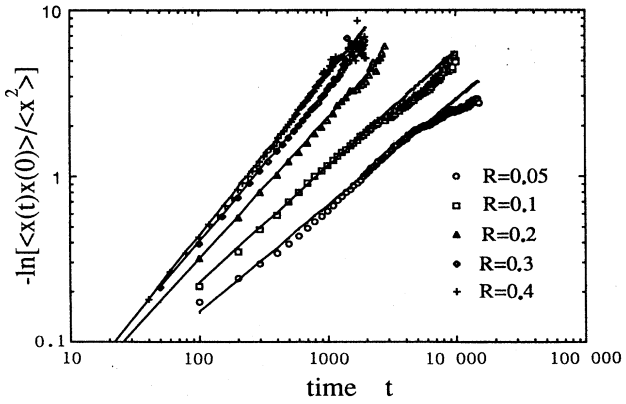

FIG. 9. Data of Fig. 8 replotted as $\ln\{-\ln[\langle x(t)x(0)\rangle/\langle x^2\rangle]\}$ vs ln$t$. The solid straight lines determine the parameters of the fitting stretched exponential $\langle x(t)x(0)\rangle/\langle x^2\rangle=e^{-(t/\tau^*)^{\beta^*}}$.

V. SUMMARY

In this paper I have extended previous work on hopping in hierarchical structures to include the effects of a background potential. The potential introduces asymmetry in the hopping rates, and a unique global minimum to which the system tries to relax. It was shown that the vanishing of an effective diffusion constant, characterizing the barrier structure, led to localization of the low-lying eigenstates of the master equation, at the most difficult barriers to cross. This localization led to a tran-

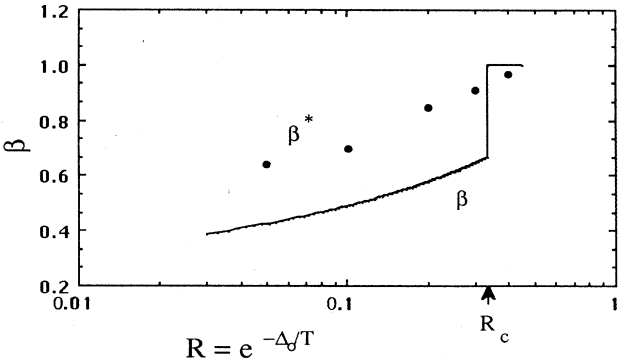

FIG. 11. Exponent β^* of the empirically fitted stretched exponentials to the data of Figs. 8 and 9. $\beta(R)$ from Eq. (4.10) is shown as a solid line for comparison.

sition from pure exponential relaxation at all times, to stretched exponential relaxation at long times.

Although the model treated here is a very specific one, the qualitative features found should apply more generally, and be of relevance to more realistic glassy systems. The specific form of the hierarchy chosen in this model played an important role in deriving the asymptotic stretched exponential relaxation in Sec. IV A. However, it was shown that this asymptotic form is generally only reached at very long times, and could in fact not be detected in the simulations of Sec. IV B. Nevertheless, even at shorter times where there are no strict arguments predicting a stretched exponential, the stretched exponential provided a reasonable fit to the numerical simulations. Similar observations have been made in other models,[13,17] and it has been noted experimentally[6] that data may often be equally well fit to the sum of a few exponentials. Thus it is unclear whether the stretched exponential form has a fundamental significance, or is merely a convenient empirical parametrization for fitting data.

To further test the sensitivity of the results to the particular hierarchy chosen, I have performed calculations of the lowest, nonequilibrium eigenvector in a related model in which the positions of the barriers are now randomly shuffled. The same qualitative features as in the hierarchical ordering were observed. For $R > R_c$, where the diffusion constant $D > 0$, this lowest eigenvector always approached the equal barrier form (2.17) as $\kappa \to 0$, irrespective of barrier order. For $R < R_c$, this eigenvector always became peaked at the most difficult barrier to cross. If this barrier happened to be located far from equilibrium, the state was well localized. If it was located within the equilibrium length $1/\sqrt{\kappa}$ it was peaked at the barrier, but more spread out. Thus the eigenstate structure remains qualitatively different in the two regions, and one would again expect to see a transition to anomalously slow decay in the correlation function at R_c.

One may question whether effects similar to those presented here will exist in higher dimensions, where the system can find paths around particularly difficult barriers. While it has been shown that, for all dimensions greater than two, asymptotic motion is always diffusive in models with short-range correlated random forces,[48] models with long-range correlated random forces can have subdiffusive asymptotic behavior in any dimension.[32,33] Thus the notion of the vanishing of an effective diffusion constant describing motion on a complicated free-energy surface may extend beyond the present one-dimensional example to more general geometries. In such cases, the idea that anomalous relaxation is associated with the localization of states in deep wells far from equilibrium, may prove to be a realistic interpretation of the phenomenon.

ACKNOWLEDGMENTS

It is a pleasure to thank E. Domany, M. E. Fisher, Y. Shapir, and T. Ziman for helpful conversations. This work was supported in part by a grant from the U.S.–Israeli Binational Science Foundation, and in part by funds provided by the Dean of the College of Arts and Science of the University of Rochester. I wish also to thank the Infrared Astronomy Group of the University of Rochester for the use of their Sun workstation.

[1]R. V. Chamberlin, G. Mozurkewich, and R. Orbach, Phys. Rev. Lett. **52**, 867 (1984); R. Hoogerbeets, W.-L. Luo, and R. Orbach, *ibid.* **55**, 111 (1985); K. Gunnarsson, P. Svedlindh, P. Nordblad, L. Lundgren, H. Aruga, and A. Ito, *ibid.* **61**, 754 (1988).

[2]S. H. Chen and J. S. Huang, Phys. Rev. Lett. **55**, 1888 (1985).

[3]F. Mezei, W. Knaak, and B. Farago, Phys. Rev. Lett. **58**, 571 (1987).

[4]G. Kriza and G. Mihály, Phys. Rev. Lett. **56**, 2529 (1986).

[5]J. Kakalios, R. A. Street, and W. B. Jackson, Phys. Rev. Lett. **59**, 1037 (1987).

[6]G. W. Scherer, J. Am. Ceram. Soc. **67**, 504 (1984); **69**, 374 (1986).

[7]P. K. Dixon and S. R. Nagel, Phys. Rev. Lett. **61**, 341 (1988).

[8]A. Ansari, J. Berendzen, S. F. Bowne, H. Frauenfelder, I. E. T. Iben, T. B. Sauke, E. Shyamsunder, and R. D. Young, Proc. Natl. Acad. Sci. USA **82**, 5000 (1985).

[9]R. W. Hall and P. G. Wolynes, J. Chem. Phys. **86**, 2943 (1987).

[10]K. L. Ngai, Comments Solid State Phys. **9**, 127 (1979); **9**, 141 (1980).

[11]I. A. Campbell, J.-M. Flesselles, R. Jullien, and R. Botet, Phys. Rev. B **37**, 3825 (1988).

[12]V. S. Dotsenko, J. Phys. C **18**, 6023 (1985).

[13]R. Riera and J. A. Hertz (unpublished).

[14]A. T. Ogielski, Phys. Rev. B **32**, 7384 (1985).

[15]D. A. Huse and D. S. Fisher, Phys. Rev. B **35**, 6841 (1987).

[16]H. Takano, H. Nakanishi, and S. Miyashita, Phys. Rev. B **37**, 3716 (1988).

[17]A. T. Ogielski, Phys. Rev. B **36**, 7315 (1987).

[18]R. G. Palmer, D. L. Stein, E. Abrahams, and P. W. Anderson, Phys. Rev. Lett. **53**, 958 (1984).

[19]J. Klafter and M. F. Shlesinger, Proc. Natl. Acad. Sci. USA **83**, 848 (1986).

[20]A. Blumen, J. Klafter, and G. Zumofen, in *Optical Spectroscopy of Glasses,* edited by I. Zschokke (Reidel, Dordrecht, 1986), p. 199.

[21]T. A. Vilgis, J. Phys. C **21**, L299 (1988).

[22]B. A. Huberman and M. Kerszberg, J. Phys. A **18**, L331 (1985).

[23]A. T. Ogielski and D. L. Stein, Phys. Rev. Lett. **55**, 1634 (1985).

[24]M. Schreckenberg, Z. Phys. B **60**, 4831 (1985).

[25]S. Grossman, F. Wegner, and K. H. Hoffman, J. Phys. (Paris) Lett. **46**, L575 (1985).

[26]G. Paladin, M. Mezard, and C. De Dominicis, J. Phys. (Paris) Lett. **46**, L985 (1985).

[27]H. Bässler, Phys. Rev. Lett. **58**, 767 (1987).
[28]B. Ries, H. Bässler, M. Grünewald, and B. Movaghar, Phys. Rev. B **37**, 5508 (1988).
[29]M. A. Tamor, Phys. Rev. B **36**, 2879 (1987).
[30]G. J. M. Koper and H. J. Hilhorst, Europhys. Lett. **3**, 1213 (1987).
[31]C. De Dominicis, H. Orland, and F. Lainée, J. Phys. (Paris) Lett. **46**, L463 (1985).
[32]J. P. Bouchaud, A. Comtet, A. Georges, and P. Le Doussal, J. Phys. (Paris) **48**, 1445 (1987).
[33]V. E. Kravtsov, I. V. Lerner, and V. I. Yudson, Zh. Eksp. Teor. Fiz. **91**, 569 (1986) [Sov. Phys.—JETP **64**, 336 (1986)].
[34]J. P. Bouchaud, A. Comtet, A. Georges, and P. Le Doussal, Europhys. Lett. **3**, 653 (1987).
[35]T. Schneider, M. P. Soerensen, A. Politi, and M. Zannetti, Phys. Rev. Lett. **56**, 2341 (1986).
[36]T. Schneider, M. P. Soerensen, E. Tosatti, and M. Zannetti, Europhys. Lett. **2**, 167 (1986).
[37]T. A. L. Ziman, Phys. Rev. Lett. **49**, 337 (1982).
[38]S. Teitel, Phys. Rev. Lett. **60**, 1154 (1988).
[39]N. G. Van Kampen, *Stochastic Processes in Physics and Chemistry* (North-Holland, Amsterdam, 1981).
[40]S. Teitel and E. Domany, Phys. Rev. Lett. **55**, 2176 (1985).
[41]A. Maritan and A. L. Stella, J. Phys. A **19**, L269 (1986); Phys. Rev. Lett. **56**, 1754 (1986).
[42]S. Teitel, D. Kutasov, and E. Domany, Phys. Rev. B **36**, 684 (1987).
[43]H. A. Ceccatto and J. S. Riera, J. Phys. A **19**, L721 (1986).
[44]T. Vilgis, J. Phys. A **20**, 757 (1987).
[45]R. Zwanzig, J. Stat. Phys. **28**, 127 (1982).
[46]P. Dean, Rev. Mod. Phys. **44**, 127 (1972).
[47]As another example of interest, we could have chosen $\kappa=\kappa_0(T-T_c)/T$. Such a model has an equilibrium phase transition at T_c, with a precursor dynamic transition at $T=-\Delta_0/\ln R_c$, provided $R(T_c)<R_c$.
[48]D. S. Fisher, D. Friedan, Z. Qiu, S. J. Shenker, and S. H. Shenker, Phys. Rev. A **31**, 3841 (1985).